Protective Coating for Components of Fossil Energy Conversion Systems

FINAL REPORT

BY

W. Sze, H. Shimizu and W. M. Gibbon
Dept. of Metals, Glass & Ceramics.

Work on this project was conducted under the auspices of the Canada Centre for Mineral and Energy Technology, Energy, Mines and Resources, Canada.

DSS FILE NUMBER : 17SQ.23440-1-9053
DSS CONTRACT SERIAL NUMBER : 1SQ81-00070
CANMET PROJECT NUMBER : 43090203
CANMET SCIENTIFIC AUTHORITY: Dr. L.V. Whiting.

11th August, 1982

ONTARIO RESEARCH FOUNDATION

SHERIDAN PARK RESEARCH COMMUNITY

MISSISSAUGA, ONTARIO, CANADA L5K 1B3 • (416) 822-4111 • TELEX 06-982311

SEP 8 1986

MICROMEDIA

54/pp

WE, THE ONTARIO RESEARCH FOUNDATION, STIPULATE THAT THIS DOCUMENT IS SUBJECT TO THE FOLLOWING TERMS AND CONDITIONS:

1. ANY PROPOSAL CONTAINED HEREIN WAS PREPARED FOR THE CONSIDERATION OF THE ADDRESSEE ONLY. ITS CONTENTS MAY NOT BE USED BY NOR DISCLOSED TO ANY OTHER PARTY WITHOUT OUR PRIOR WRITTEN CONSENT.
2. ANY TESTING, INSPECTION OR INVESTIGATION PERFORMED BY US WILL BE CONDUCTED IN ACCORDANCE WITH NORMAL PROFESSIONAL STANDARDS. NEITHER WE NOR OUR EMPLOYEES SHALL BE RESPONSIBLE FOR ANY LOSS OR DAMAGE RESULTING DIRECTLY OR INDIRECTLY FROM ANY DEFAULT, ERROR OR OMISSION.
3. ANY REPORT, PROPOSAL OR QUOTATION PREPARED BY US REFERS ONLY TO THE PARTICULAR MATERIAL, INSTRUMENT OR OTHER SUBJECT REFERRED TO IN IT. NO REPRESENTATION IS MADE THAT SIMILAR ARTICLES WILL BE OF LIKE QUALITY.
4. NO REPORT ISSUED BY US SHALL BE PUBLISHED IN WHOLE OR IN PART WITHOUT OUR PRIOR WRITTEN CONSENT.
5. OUR NAME SHALL NOT BE USED IN ANY WAY IN CONNECTION WITH THE SALE, OFFER OR ADVERTISEMENT OF ANY ARTICLE, PROCESS OR SERVICE.
6. WE RESERVE THE RIGHT NOT TO COMMENCE AND/OR CONTINUE ANY WORK UNTIL PAYMENT ARRANGEMENTS SATISFACTORY TO US ARE ESTABLISHED.

SUMMARY

Because of the extremely aggressive environment generated in coal conversion systems, particularly direct-fired fluidized beds, some of the components must be given a protective coating if costly breakdowns are to be be avoided. During the past year, ORF has undertaken an investigation in which titanium diboride (TiB_2) coatings up to 50μm thick have been deposited, by means of Chemical Vapour Deposition (CVD), on sheet coupons of some alloys used, or of potential use, in coal conversion systems. Bending, thermal fatigue and aqueous solution corrosion testing were performed successfully, but because of edge effects apparently associated with the specimen shape, corrosion testing at elevated temperature in an SO_2-bearing atmosphere could not be carried out. However, the results are sufficiently encouraging that further work is recommended in which the specimen shape will be changed.

TABLE OF CONTENTS

		Page No.
1.	INTRODUCTION	1
2.	EXPERIMENTAL PROCEDURE	
	2.1. Substrate Materials	2
	2.2. Reactant Materials	3
	2.3. Apparatus	3
	2.4. Substrate Preparation and Coating Procedures	4
	2.5. Structural Examination.	5
	2.6. Corrosion Test (Coating porosity)	5
	2.7. Adhesion Evaluation	5
	2.8. Thermal Cycling	5
	2.9. Erosion Test	6
3.	RESULTS AND OBSERVATIONS	
	3.1. Substrate Coatability	6
	3.2. Coating Composition and Morphology.	7
	3.3. Coating/Substrate Interface Microstructure.	8
	3.4. Corrosion Test (Coating Porosity)	8
	3.5. Adhesion Evaluation	9
	3.6. Other Evaluations	9
4.	DISCUSSION	
	4.1. Substrate Preparation and Coatability	9
	4.2. Deposition Parameters	11
	4.2.1. Operating Pressure	11
	4.2.2. Temperature	11
	4.2.3. Reactant Gas Flow Rate	12
	4.2.4. Reactant Gas Composition and B/Ti Ratio	12
	4.3. Gas Flow Pattern	13

Cont...

TABLE OF CONTENTS - Continued

Page No.

4.4. Coating Morphology 14
4.5. Coating Evaluation 14
5. CONCLUSIONS 15
6. RECOMMENDATION 16
REFERENCES 17
LIST OF TABLES
LIST OF FIGURES
LIST OF APPENDICES

1. INTRODUCTION

Advanced engineering applications often demand materials which can perform under aggressive environmental conditions without suffering from a loss of bulk strength and specific surface properties. As the material performance requirements become more stringent, it becomes more impractical for a single material to satisfy all the diverse technical and economic requirements. Coating technology offers an attractive option of choosing a base material for purely economic reasons.

Protective coatings which can resist corrosive and erosive environments are particularly useful in coal conversion systems. Higher operating temperatures which increase the conversion efficiency will generally aggravate the material problems[1]. Refractory coatings which are known for their superior performance under such conditions compared with most metals, require special coating techniques because of their higher melting temperatures. Chemical vapour deposition (CVD) provides a technique for obtaining coatings of refractory materials[2][3][4].

The CVD process utilizes gaseous phase chemical reactions to deposit solid materials on hot substrate surfaces. A wide range of metallic and ceramic coatings, including those refractory metals which for reasons of either chemistry, brittleness or high melting point, cannot be readily deposited by other methods, can be deposited by CVD. It enables thin dense coatings to be applied to components with complex-shaped internal surfaces. The versatility of the CVD process and products makes it potentially very useful for applying protective coatings to components of coal utilization and conversion plants.

Titanium diboride (TiB_2) is a stable high melting temperature (3000°C) refractory material with excellent thermal stress resistance, i.e. high thermal conductivity (0.058 cal/cm. sec°C) and low thermal expansion (5.6 - 6.6 ppm/°C)[5]. It is an extremely hard material (3400 VHN),

.../2

much harder than WC (2400 VHN). It retains a higher hardness value at high temperatures, and has a better oxidation resistance than carbides and nitrides[5][6][7]. It has good chemical resistance at high temperature against most acids, molten metals and non-basic slags and salts[5][8]. CVD coatings of TiB_2 have already been used successfully on letdown valves in a bench scale coal liquefaction reactor at Sandia Laboratories[9], and appear to have the potential of providing corrosion and erosion protection to components of coal conversion furnaces.

During the past nine months, Ontario Research Foundation has been investigating the technical feasibility of applying CVD TiB_2 coatings to some of the alloys used, or of potential use, in coal conversion systems. The experimental work and results of this investigation are summarized in this final report.

2. EXPERIMENTAL PROCEDURE

2.1. Substrate Materials

CVD TiB_2 coatings were applied to small sheet specimens of the following alloys to test the feasibility of coating a variety of substrate materials.

AISI 1040 Carbon Steel
AISI 1018 Carbon Steel
Type 430 Ferritic Stainless Steel
Type 410 Martensitic Stainless Steel
Type 304 Austenitic Stainless Steel
Type 316 Austenitic Stainless Steel
Inconel 601
Cobalt-Chromium Alloy

The details of the substrate specimens and the alloy compositions are given in Appendix A.

.../3

2.2. Reactant Materials

The reactant materials consisted of the following chemicals:

- Titanium tetrachloride liquid held at an appropriate temperature.
- Boron trichloride compressed vapour at room temperature.
- Hydrogen as a carrier gas and a reducing agent.

In addition, argon was used to sweep out the reaction chamber before and after coating. The specifications for these chemicals are listed in Appendix B.

2.3. Apparatus

The CVD apparatus was based on the "cold-wall" principle, most conveniently applied in practice by means of induction heating. Two types of cold-wall reaction chamber were investigated during the course of this project. The majority of the experiments were carried out using a 51mm diameter quartz tubing surrounded with an induction coil. The other type consisted of a 254mm diameter water-cooled metal chamber with an induction coil mounted inside it.

Figure 1 is a schematic diagram of the CVD circuit with the quartz reaction chamber. The overall arrangement of the metal chamber installed in the same CVD circuit is shown in a photograph in Figure 2. The tubular graphite susceptor is shown in Figure 3, and a close-up view of the induction coil installed in the metal chamber is shown in Figure 4. The susceptor temperature was controlled by adjusting the output of a Lepel 10KW induction generator connected to a copper induction coil which provided a 75mm heating zone. The temperature of the liquid $TiCl_4$ was controlled at $45^{\circ}C$ by means of a water bath. The line between the $TiCl_4$ reservoir and the reaction chamber was kept at above

.../4

45°C with heating tapes, to maintain the correct $TiCl_4$ vapour pressure in the reaction chamber.

The details of the various components of the CVD circuit as well as other details of the two types of chamber and the specifications of the Lepel 10KW induction generator, are listed in Appendix C.

2.4. Substrate Preparation and Coating Procedures

The coupons, 30mm x 25mm, were cut from the various sheet materials. The corners and edges were ground off, then the surfaces were sandblasted with #36 grit Al_2O_3 and ultrasonically cleaned. The coupons were weighed to 0.1 mg.

Each coupon was placed upright in the centre of the graphite susceptor in the middle of the heating zone. The reaction chamber and gas lines were then flushed with argon for two hours, followed with hydrogen. The temperature in the susceptor was raised and held at 927°C in hydrogen to clean the substrate. When the temperature had stabilized, the valves of the $TiCl_4$ reservoir were opened to allow a hydrogen gas flowrate of 890 ml/min through the reservoir to carry the required amount* of titanium tetrachloride vapour into the reaction chamber. The gas flow of boron trichloride was adjusted to a 4.3 - 6.9 ml/min range in order to maintain the B/Ti ratio in the 0.13 - 0.2 range. The deposition of TiB_2 was based on the following reaction.

$$TiCl_{4(g)} + 2BCl_{3(g)} + 5H_{2(g)} \longrightarrow TiB_{2(s)} + 10HCl_{(g)}$$

After 2-3 hours of deposition, the reactant gases were shut-off and the system was flushed with hydrogen to remove residual gaseous products and to prevent the reverse reaction during cooling. The substrate was weighed to determine the weight gain, from which the

.../5

* For details of vapour pressure calculations etc., see Appendix D.

coating thickness could be estimated based on the density of TiB_2. (4.52 gm/cm^3)

2.5. Structural Examination

The surface of the CVD TiB_2 coating was examined under the scanning electron microscope. Selected coated specimens were mounted, cross-sectioned and polished using a dull 600 emery paper in the final polishing, to retain the integrity of the hard coating[10]. The coating and the interface between the coating and the substrate were then examined metallographically.

2.6. Corrosion Test (Coating porosity)

The coated specimens (1040 C.S., 430 S.S., 410 S.S., and 304 S.S. dull Ni plated) were examined for microporosity by subjecting them to corrosion testing. The edges of all specimens to be tested were covered with paraffin wax to protect the imperfectly coated edge areas. Coated and uncoated specimens were immersed in a 10% H_2SO_4 solution at 23°C for 48 hours. The solution was changed after 24 hours and the specimens were weighed before and after each immersion.

2.7. Adhesion Evaluation

Coated specimens 0.76mm thick (1040 C.S., 430 S.S., and 304 S.S.) were bent to an included angle of approx. 120° and 1.83mm thick specimens (410 S.S.) to an included angle of approx. 30°. All bent specimens were examined visually for signs of cracking and peeling.

2.8. Thermal Cycling

Coated specimens of 1040 C.S., 430 S.S., 410 S.S. and 304 S.S. were flame heated to a red-hot state (approx. 700°C) and cooled to room temperature. This cycle was repeated ten times before quenching the red-hot specimens into water. The specimens were examined visually for signs of spalling.

.../6

2.9. Erosion Test

Coated and uncoated specimens of 1040 C.S., 430 S.S. and 410 S.S. were sandblasted over a 10mm dia. area with 100-500 grams of #60 grit SiC at 30mm distance, using a 200-600kpa air presssure and a 8mm dia. orifice. The specimens were ultrasonically cleaned and weighed before and after each test. Weight loss defined the degree of erosion of the coated and uncoated specimens.

3. RESULTS AND OBSERVATIONS

3.1. Substrate Coatability

A substrate material was classed roughly as either coatable or not coatable, depending on whether or not the TiB_2 coating could be successfully deposited on it. The appearance of a coated specimen was a good indication of the coating quality; a good coating generally appeared uniformly metallic grey, while a poor coating appeared uneven and spotty. Quantitatively, well coated specimens showed consistently higher weight gain, while poorly coated specimens showed much less weight gain.

TiB_2 coatings applied directly on 1040 C.S., 1018 C.S., 430 S.S. and 410 S.S. were dense and smooth and a weight gain of about 300mg was reasonably consistent. Therefore, these alloys were considered to be coatable. On the other hand, TiB_2 coatings applied directly on 304 S.S., 316 S.S., Inconel 601 and Co-Cr alloy, were spotty, and the weight gain was under 100mg. Therefore, these alloys were considered to be uncoatable.

The 304 S.S. plated with electro-deposited dull nickel was coated with TiB_2. The coating was smooth and the weight gain by the specimen was about 400mg, but a TiB_2 coating on an electroless nickel plated 304 S.S. substrate was flaky and the weight gain was under 300mg.

.../7

The results of coating the different alloys are summarized in Table 1 and the deposition parameters used are tabulated in Table 2. Those specimens subjected to various qualitative tests, are listed in Table 3. The deposition parameters and coating results for all the specimens tested, are listed in Appendix E.

3.2. Coating Composition and Morphology

The first step in evaluating the quality of a TiB_2 coating was to determine its composition by X-ray diffraction. It showed TiB_2 was the only compound present in the coating. The surface structure of the coating was then studied. It was found that the coating often showed surface markings, and the general appearance was different in different regions (A, B & C) of the coated specimens of 1040 C.S., 430 S.S. and 410 S.S., as illustrated in Figure 5. When these regions were examined under the SEM, Region A which appeared shiny macroscopically, was seen to be composed of the spherically shaped crystals shown in Figure 6. Region B, which appeared generally metallic, was composed of spherical/nodular crystals which appeared typically as in Figure 7. Region C appeared dark and flaky. It was seen to have the structure shown in Figure 8, and contained pin-holes.

The coating on 304 S.S. with a dull nickel intermediate layer, had similar surface markings to those observed on the other substrate materials, but the SEM structure was uniform for any one specimen, and did not show variations such as those in Figures 6, 7 and 8. Two distinct growth morphologies were observed in these specimens, i.e. spherical (shiny) and crystalline (dull). A shiny coating had a smooth spherical structure (Figure 9) and a crystal-like coating had a cubical structure (Figure 10). The variables affecting the coating structure are unknown at this time.

.../8

3.3. Coating/Substrate Interface Microstructure

Metallographic examination of the interface between the coating and the substrate revealed the coating quality and integrity. Longitudinal sectioning of a coated specimen (Figure 11) showed the coating thickness distribution along the substrate. On one side of the specimen, the coating was even and remained adhered to the substrate, but the metallographic specimen preparation procedure unavoidably caused some damage to the coating on the opposite side. The interface microstructures of coated 1040 C.S., 410 S.S. (similar to 430 S.S.) and 304 S.S. with dull-Ni plating, are shown in Figures 12, 13 and 14 respectively. The interfaces were sound and free of voids. A typical poor quality TiB_2 coating on a 1040 C.S. substrate, with a porous Fe_2B interface, is shown in Figure 15. The porosity at the interface was eliminated by lowering the B/Ti ratio in the reactant gas composition from 0.20 to 0.13. Scanning electron micrographs of the above mentioned coating and substrate interfaces are shown in Figures 16, 17, 18 and 19. With the improved depth of field, the SEM photos showed the quality of the interfaces more clearly.

3.4. Corrosion Test for Evaluation of Coating Porosity

Microscopic examination of the coating was useful in demonstrating the soundness of the coatings, but the quality of the coating was further evaluated by corrosion testing. A good quality coating was free of microcracks and pin-holes, and protected the substrate from corrosion.

The appearance of the specimens after the corrosion test is shown in Figure 20 (a) and (b). Bare 1040 C.S. suffered severe corrosion attack and the 0.76mm thick specimen was almost completely penetrated through. Bare 430 S.S. and bare 410 S.S. showed some degree of surface corrosion. Bare 304 S.S. had negligible surface corrosion, while the dull Ni plated 304 S.S. had some spotty discoloration in the nickel plating. In contrast, the TiB_2 coated specimens showed

.../9

no sign of corrosion attack. The detailed measurements of the weight loss by the specimens are included in Table 4.

3.5. Adhesion Evaluation

The quality of bonding between coating and substrate was evaluated by bend testing coated specimens. As shown in Figure 21, Most of the outer surface coating on the thick specimens (410 S.S.) peeled off, but the coating on the thin specimens of 1040 C.S., 430 S.S. and 304 S.S. with dull Ni plating remained adhered, except at the edges, where spalling was suspected. All the coatings on the inner surface of the specimens peeled off during bending. Severe bending produced hairline cracks on the outer surface of thin specimens, but the coating remained adhered to the substrate.

3.6. Other Evaluations

Simple thermal cycling tests and erosion tests were carried out with coated specimens. The color of the specimens subjected to thermal cycling tests changed to bluish grey, but all the coatings remained tightly adhered to the substrates even after several heating and quenching cycles. Erosion test results on the coated and uncoated substrates showed no significant difference in weight loss.

4. DISCUSSION

4.1. Substrate Preparation and Coatability

The adhesion of a coating to a substrate depends upon the mechanical and chemical properties at the interface, such as mechanical interlocking and diffusion of species between the coating and the substrate.

.../10

Inter-diffusion will generally benefit coating adhesion, but diffusion which produces brittle intermetallic compounds may weaken the interface, leading to coating failure. A hard, brittle interlayer can accomodate little stress and therefore, has a weak bonding effect. On the other hand, a soft, ductile interface can accomodate more stress and will improve the strength of bonding.

In this investigation, it was found that the adhesion of CVD TiB_2 coatings to 1040 carbon steel was better on a sandblasted surface than on a fine polished surface. Although the surface appearance on a fine polished surface was smooth, the coating peeled off the substrate. On the sandblasted surface, the coating seemed rougher, but the adhesion was superior. It is believed that mechanical anchoring of a coating to the substrate at the interface, is an important parameter in coating adhesion[11].

Some degree of diffusion at the interface is present in all CVD processes, but the success achieved in coating various substrate materials depends also upon matching the thermal expansion coefficient of the substrate to that of TiB_2[5][12]. TiB_2 has a relatively low thermal expansion coefficient (5.6 - 6.6 ppm/^{o}C) compared with those of the substrate materials studied in this investigation. A difference in the expansion rates will result in residual stress during cooling, and if the stress is sufficiently large, the coating will crack and spall off. Substrates such as Kovar (28% Ni, 18% Co, 54% Fe), tantalum, cemented WC and cemented TiC whose thermal expansion coefficients (5-7.5 ppm/^{o}C) are closely matched with that of TiB_2, are reported to have been successfully coated with CVD TiB_2 without spalling[5][12]. In this investigation, sheet materials of 1040 C.S., 1018 C.S., 430 S.S. and 410 S.S. with thermal expansion coefficients in the range of 10 ppm/^{o}C were coated with TiB_2 except at the sharp edges where spalling

.../11

occurred. Substrate materials 304 S.S., 316 S.S., Inconel 601, and Co-Cr alloy, with higher thermal expansion coefficients (16 ppm/^{o}C) could not be coated.

It is significant that a soft ductile material, like electro deposited dull nickel (thermal expansion coefficient 13.3 ppm/^{o}C) enabled 304 S.S. to be coated by accomodating the thermal stress during cooling without damaging the coating, while harder electroless plated nickel on 304 S.S. did not have the same effect.

4.2. Deposition Parameters

Deposition parameters are known to affect both the deposition rate and the quality of the coating[5][12][13]. Under the CVD conditions investigated, TiB_2 and boron are the only solids which can deposit on the substrates[14][15].

4.2.1. Operating Pressure

The operating pressure was held at one atmosphere all through the investigation to eliminate the need for complex vacuum equipment.

4.2.2. Temperature

Higher operating temperatures increased the deposition rate but the coating tended to deposit heavily at the front end of the substrate (facing the gas inlet) and left the rear end barely covered. The thickness uniformity was improved at a lower temperature. An operating temperature of 927^{o}C was chosen in order to have a sufficient deposition rate with a relatively even coating thickness distribution.

.../12

4.2.3. Reactant Gas Flow Rate

Hydrogen was the reducing gas as well as the carrier gas for the $TiCl_4$. Both the hydrogen and the titanium tetrachloride flowrates had little effect on the deposition rate, but a certain amount of hydrogen flow was required to maintain a reducing atmosphere and to prevent a reverse chemical reaction during cooling. The hydrogen flow rate was primarily governed by a requirement that a certain minimum volume of $TiCl_4$ was needed to assure complete coating coverage of the substrate*.

The boron trichloride flow rate affected the deposition rate; increasing the BCl_3 flow rate (from 4.3 ml/min to 6.9 ml/min) increased the deposition rate noticeably. (from 50 mg/hr. to 150 mg/hr.)

Since the hydrogen flow rate and the temperature of the $TiCl_4$ chamber water bath were fixed at 890 ml/min and 45°C, the boron flow rate was the only means of controlling the reactant gas composition.

4.2.4. Reactant Gas Composition and B/Ti Ratio

The coating quality was extremely sensitive to the gas composition, in particular the ratio between the BCl_3 and the $TiCl_4$ carried by the hydrogen, i.e. the B/Ti ratio. Thus, the ratio of the flow rate of hydrogen to the flow rate of BCl_3 had to be adjusted carefully. The flowmeter used (ball type) was somewhat inadequate for fine tuning the low flow rate of BCl_3 required in this investigation. A high BCl_3 flow rate resulted in a higher deposition rate of sound TiB_2 up to a point. However, when the boron concentration was too high a porous coating resulted. This

* Efficiency of TiB_2 Formation - see Appendix "F"

.../13

observation was also reported by T. Takahashi[13]. It was concluded that the reactant gas composition must be very carefully monitored and controlled to obtain high quality TiB_2 coating. In the case of the 1040 C.S. substrate, for example, it was found that as the B/Ti ratio was increased to beyond 0.2, porosity appeared at the interface between the TiB_2 and the steel. This was eliminated completely by adjusting the B/Ti ratio appropriately. It was thus confirmed that the porosity resulted from an inappropriately high concentration of boron and the resulting mass imbalance caused by the formation of a Fe_2B phase at the interface.

The B/Ti ratios were kept in the range of 0.13 - 0.2 for the difference substrate materials studied.

4.3. Gas Flow Pattern

The visual appearance of the coating on the substrate seemed to reflect the pattern of gas flow. Experiments were carried out to eliminate this flow pattern. Specimens were placed at different locations and orientations inside the graphite susceptor, i.e. standing vertically at various distances away from the gas inlet of the susceptor or placed in a different orientation with respect to the flow axis, i.e. parallel or perpendicular. A parabolic flow pattern was reproduced in all the locations. The height and the diameter of this parabolic pattern were believed to be affected by the geometry of the gas entry end of the hollow graphite susceptor. A large metal chamber was used to study the possibility of replacing the gas flow dynamics with a diffusion type of environment. Results indicated that the new arrangement still did not provide a perfect diffusion condition.

.../14

4.4. Coating Morphology

The flow pattern on the specimens seemed to delineate a boundary between the good coating (inside the conical envelope) and the poor coating (outside the envelope). The two had a distinctive deposition structure. The coating at the front end of a specimen (within the boundary of the flow pattern) appeared shiny or metallic grey and, under SEM, its structure was seen to be nodular and spherical (Figures 6 and 7). No void was observed in this region. This kind of coating morphology was similar to those reported by others[5][12]. The coating at the rear end of a specimen, e.g., the region C in the specimen shown in Figure 5, appeared dull and dark visually, and under SEM, the structure was found to be crystalline with planar edges (Figure 8). Voids were found in this region. This kind of coating morphology has not been reported by other investigators.

4.5. Coating Evaluation

The coatings showed excellent corrosion resistance against 10% H_2SO_4 at room temperature, good adhesion to the substrate, as well as considerable thermal shock resistance. Only the edges, where spalling was suspected, showed signs of weakness.
Two 1040 C.S. specimens sent to CANMET were tested in an atmosphere containing 2000 ppm of SO_2, at 900°C for 300 hours. These two specimens disintegrated totally during the test. It was believed that the corrosion attack originated from the edges because of the poor edge coverage by TiB_2, and penetrated through the substrate material.

.../15

5. CONCLUSIONS

5.1. If the thermal expansion coefficient of the substrate is more than twice that of the TiB_2 coating, the quality and adhesion of the coating are poor, and the substrate is considered to be "uncoatable". However, if the ratio of the thermal expansion coefficients is between one and two, satisfactory coatings can be deposited directly on the substrate.

5.2. Substrates considered to be "uncoatable", e.g. 304 S.S., 316 S.S., Inconel 601 and cobalt-chrome alloy can be coated satisfactorily with TiB_2 if they are electro-plated with dull nickel.

5.3. The soundness of the interface between the coating and carbon steel is sensitive to the boron concentration in the gas phase. Excess boron favours the formation of an iron boride compound (Fe_2B) and results in porosity along the interface. The gas composition, in particular the B/Ti ratio, is critical in the production of sound dense coating on 430 ferritic stainless steel series, even though these materials do not appear to be prone to porosity formation.

5.4. Sound coatings can be produced on the flat region of a sheet specimen. The edges cannot be coated properly, because of the suspected thermal stress effects.

.../16

5.5. The coating quality appears to depend on, among other factors, the gas flow characteristics on and around the substrate. The best quality coating was deposited on the region of the substrate nearer the gas entry end of the reaction chamber.

5.6. Sound coatings show excellent corrosion resistance to sulphuric acid solution, good adhesion to the substrate and good thermal shock resistance.

6. RECOMMENDATION

One of the objectives of this investigation was to supply specimens to CANMET for corrosion testing in a hot SO_2 atmosphere. This was not possible because of the edge effect encountered when coating thin sheet specimens. Therefore, it is recommended that a second stage of the investigation be undertaken, in which specimens of a shape designed to eliminate edge effects will be coated with CVD TiB_2 and submitted to CANMET for hot corrosion testing.

W.M. Gibbon, P.Eng.,
Assistant Director,
Dept of Metals, Glass & Ceramics.

H. Shimizu, Ph.D.,
Research Scientist,
Dept. of Metals, Glass & Ceramics

William Sze, P.Eng.,
Associate Research Scientist,
Dept. of Metals, Glass & Ceramics

:lju
encl.

REFERENCES

1. A.J. MacNab, Report on Corrosion and Erosion at High Btu Gasifier Components, Metal Progress Nov.1977 p.44-49.

2. K.K. Yee, Protective Coatings for Metals by Chemical Vapour Deposition. International Metals Review, 1978 No. 1 p.19-42.

3. N.J. Archer, Chemical Vapour Deposition, Phys. Technol. Vol. 10 1979 p.152-161.

4. Materials Coating Techniques, AGARD-LS-106, 1980.

5. H.O. Pierson and E. Randich, Proceedings of the 6th International Conference on C.V.D., 1977. p.304-317

6. E. Randich, C.V.D. Boride Coatings for Erosion Applications NTIS CONF-790903-1 (SAND-78-2294C).

7. W.D. Kingery, J. Am. Cerm. Soc. 38.1 (1955) p.1-14.

8. R. Thompson, J. of Less Common Metals 47(1976) p.279-282.

9. E. Randich, 3rd Annual Conference on Materials for Coal Conversion and Utilization III-55, Oct. 10-12, 1978.

10. M.E. McAllaster, Metallographic Preparation of Titanium Diboride Coatings, SAND-80-0596, 1980.

11. H.O. Pierson, E. Randich and D.M. Mattox, J. of Less Common Metals 67(1979) p.381-388.

12. H.O. Pierson, E. Randich, Thin Solid Film 54 (1978) p.119-128.

13. T. Takahashi and H. Kamiya, J. Crystal Growth 26(1974) p.203-209.

14. T.M. Besmann and K.E. Spear, J. Electrochemical Society 124(5)(1977) p.786-790.

15. T.M. Besmann and K.E. Spear, J. Electrochemical Society 124(5)(1977) p.790-797.

LIST OF TABLES

TABLE 1 : CVD TiB_2 Coating on Alloys

2 : Coating Parameters

3 : List of Tested Samples

4 : Corrosion Test Results

TABLE 1

CVD TiB_2 COATING ON ALLOYS

SUBSTRATES	SATISFACTORY COATING
1040 Carbon Steel	Yes
1018 Carbon Steel	Yes
430 Ferritic Stainless	Yes
410 Martensitic Stainless	Yes
304 Austenitic Stainless	No
304 S.S. Electroless Ni Plated	No
304 S.S. Electro-plated Ni (dull)	Yes
316 Austenitic Stainless	No
Inconel 601	No
Cobalt-Chromium Alloy	No

TABLE 2

COATING PARAMETERS

PARAMETERS	CONDITIONS
Substrate Preparation	30mm x 25mm sheet, corners and edges ground off, sandblasted with #36 grit Al_2O_3, ultrasonically cleaned.
Temperature	927°C
Pressure	760mm Hg
H_2 flowrate	890 ml/min
BCl_3 flowrate	4.3 - 6.9 ml/min
$TiCl_4$ Chamber	at 45°C, 34.2 ml/min of $TiCl_4$ vapour with H_2 flowing at 890 ml/min.
H_2: $TiCl_4$: BCl_3 gas composition	96: 3.5: 0.5 (approx.)
B: Ti ratio	0.13 - 0.2
H/Cl ratio	11.3 - 11.9
Coating Duration	2 - 3 hours.
Rate of Coating	100mg/hr (15µm/hr)

TABLE 3

LIST OF TESTED SAMPLES

Alloy	Spec.No.	Coating thickness wt.(mg)	est. thick.(μm)	Test Performed	Remarks
1040	49 (Prelim)	325	30	Metallography & SEM X-ray diffraction	
Carbon Steel	53 (Prelim)	N.A.	30	Bending	
	2	195	30	Sent to Canmet	
	4	258	40	Sent to Canmet	
	9	276	40	Bending	
	13	184	30	Thermal Cycling	
	14	270	40	Erosion	
	16	318	45	Sent to NRC	
	17	N.A.	45	Corrosion	
	26	417	60	Metallography & SEM.	Porous Fe_2B
430 Ferritic Stainless Steel	B7	217	30	Thermal cycling	
	B9	284	40	Metallography & SEM	
	B10	354	55	Sent to NRC	
	B13	208	30	Bending	
	B19	244	35	SEM	gas flow pattern and flaky coating
	B23	281	40	Erosion	
	B24	291	45	Corrosion	
	B27	237	35	Bending	
	B28	294	45	Erosion	
	B33	271	40	Thermal cycling	
410 Martensitic Stainless Steel	C1	238	35	Bending	
	C2	327	50	Metallography & SEM	
	C3	334	50	Corrosion	
	C4	332	50	Erosion	
	C5	324	50	Erosion	
	C6	196	30	Thermal cycling	
	C7	169	25	Bending	
	C9	225	35	Erosion	
304 (Ni) Austenitic Stainless Steel dull Ni plated (10-20μm)	N1	207	30	Bending	shiny coating
	N2	317	45	Corrosion	" "
	N3	302	45	Metallography & SEM	" "
	N4	246	35	Metallography & SEM	crystal-like coating
	N5	470	70	Thermal cycling	" "
	N6	434	65	Bending	" "

TABLE 4

CORROSION TEST RESULTS

SAMPLE	Rate of Penetration mg/mm^2 - 48 hrs.	Degree of Penetration in comparison with 1040 C.S.
1040 C.S. uncoated	4.3	100%
1040 C.S. TiB_2 coated	.006	0.1%
430 S.S. uncoated	2.5	55%
430 S.S. TiB_2 coated	.005	0.1%
410 S.S. uncoated	1.5	35%
410 S.S. TiB_2 coated	.001	0.02%
304 S.S. uncoated	.016	0.4%
304 S.S. dull Ni plated	.004	0.1%
304 S.S. dull Ni plated and TiB_2 coated	.001	0.02%

Test Conditions: 10% H_2SO_4 at 23°C for 48 hours, solution changed every 24 hours.
Sample edges protected by paraffin wax

C.S. - Carbon Steel

S.S. - Stainless Steel

LIST OF APPENDICES

APPENDIX A : List of Substrate Materials

B : List of C.V.D. Chemical Reactant Materials

C : List of Apparatus

D : Flow Rate of Titanium Tetrachloride

E : Results of CVD TiB_2 Coating, including Preliminary Runs

F : Efficiency of TiB_2 Formation

APPENDIX A

List of Substrate Materials

Alloy	Composition	Dimensions (W x L x t)
Carbon Steel 1040	0.40% C, 1.2% Mn	30mm x 25mm x 0.76mm
Carbon Steel 1018	0.18% C, 0.8% Mn	30mm x 25mm x 3.18mm
Ferritic Stainless Steel 430	0.12% C, 1.0% Mn, 16-18% Cr	30mm x 25mm x 0.76mm
Martensitic Stainless Steel 410	0.15% C, 1.0% Mn, 11.5%-13.5% Cr	30mm x 25mm x 1.83mm
Austenitic Stainless Steel 304	0.08% C, 2.0% Mn, 18-20% Cr, 8-10.5% Ni	30mm x 25mm x 0.76mm
Austenitic Stainless Steel 316	0.08% C, 2.0% Mn, 16-18% Cr, 10-14% Ni, 2-3% Mo	33mm x 32mm x 0.76mm
Inconel 601	0.03% C, 0.3% Mn, 14.7% Fe, 61% Ni, 22.1% Cr	30mm x 25mm x 3.18mm
Cobalt-Chromium alloy	27-30% Cr, 5-7% Mo, 0-2.5% Ni, Balance Co	irregular rectangular

APPENDIX B

List of C.V.D. Chemical Reactant Materials

a) Titanium tetrachloride: - Purified grade liquid, held in a 45°C water bath, line between reaction chamber and $TiCl_4$ chamber heated up to 100°C to ensure $TiCl_4$ vapour maintained at 45°C saturated level.

b) Boron trichloride: - Compressed vapour (4 psig) in liquid phase (99.9% min.)

c) Hydrogen: - Prepurified 99.95% min.

d) Argon: - Prepurified 99.998% min.

APPENDIX C

List of Apparatus

a)	R.F. Generator:	"Lepel" model T-10-3-DF-TL, 10KW capacity, 200-450 kHz. rf. range
b)	Quartz Chamber:	51mm I.D. quartz tube, fitted with stainless steel end caps sealed with viton "O" rings, Chromel-Alumel thermo-couple, graphite susceptor, stainless steel heat baffle.
c)	Metal Chamber:	25.4cm I.D. x 41cm length water cooled cold wall copper and bronze chamber, fitted with nylon and bronze end caps sealed with "O" ring, a copper work coil, Chromel-Alumel thermo-couple, graphite susceptor using a quartz tube as a barrier.
d)	Graphite Susceptor:	45mm O.D. dumb-bell shaped with a 25mm high x 30mm wide hollow square and a 6mm semi-circular groove in the top and bottom at the centre.
e)	Titanium Tetrachloride Reservoir:	500ml gas wash bottle immersed in water bath, top section and exit end heated with flexible heating tape.
f)	Discharge System:	Glass wool filter, ice water trap, drierite dryer, water scrubber.
g)	Overall Coating System:	Pressure gauges, gas flowmeters, stainless steel needle valves and fittings, teflon on/off valves, 6mm teflon tubing, nylon joints, short polyethylene tubing sections, rubber stoppers, flasks.

APPENDIX D

Flow Rate of Titanium Tetrachloride

Vapour pressures P(mmHg) of titanium tetrachloride at various temperatures T (^{o}K) are calculated from the following equation:

$$\log P = -2{,}919T^{-1} - 5.788 \log T + 25.129$$

At 45^{o}C, the vapour pressure of titanium tetrachloride is 29.22mmHg. Assuming an ideal gas law, at constant temperature the gas volume is proportional to its partial pressure. For a hydrogen carrier gas flow rate of 890 ml/min, the flow rate of $TiCl_4$ is determined as follows:

$$\frac{F_1}{F_2} = \frac{P_1}{P_2}$$

$$F_1 = \frac{P_1}{P_2} \times F_2$$

$$= \frac{29.22\text{mmHg}}{760\text{mmHg}} \times 890 \text{ ml/min}$$

$\therefore$ $TiCl_4$ Flow Rate = 34.2 ml/min

(1) Data from O. Kubaschewski, E.Ll. Evans, C.B. Alcock Metallurgical Thermochemistry, 1967.

APPENDIX E - RESULTS OF CVD TiB_2 COATING (Preliminary Runs)

Substrate Materials: 1040 C.S. (0.4%C, 1.2%Mn)

Substrate Dimensions: (width x length x thickness) 33.3mm x 31.8mm x 0.79mm

Spec. No.	Surface Preparation	Temp. °C	H_2 flow ml/min.	BCl_3 flow ml/min.	$TiCl_4$ Temp. °C	$TiCl_4$ Flow ml/min.	Duration Hr.	Wt. Gain mg.	Remarks
1)	240 Emery Paper	1000	866	14	23	10,4	2	NA	Crystal-like incompletely coated
2)	600 Emery Paper	1000	866	14	23	10.4	2	NA	
3)	Boiled KOH solution	1000	866	14	23	10.4	2	NA	
4)	60 Emery Paper	870	866	22	23	10.4	2	144	Even TiB_2 and Fe_2B (porous) coating
5)	180 Emery Paper	870	866	22	23	10.4	2	158	
7)	60 Emery Paper	870	866	22	23	10.4	2	159	
6)	SB#36 Al_2O_3 80p.s.i.	925	866	42	23	10.4	2	204	Improved coating adhesion
8)	" " 60p.s.i.	925	866	42	23	10.4	2	325	
9)	" " 90p.s.i.	925	866	42	23	10.4	2	319	
10)	SB#36 Al_2O_3 60p.s.i.	970	866	92	23	10.4	2	285	
11)	" " 80p.s.i.	970	866	42	23	10.4	2	264	Crystal-like coating
12)	" " 95p.s.i.	970	866	42	23	10.4	2	318	
13)	SB#36 Al_2O_3 60p.s.i.	915	400	37	23	4.5	2	63	
14)	" " 80p.s.i.	915	400	37	23	4.5	2	94	Reduced gas flow pattern
15)	" " 95p.s.i.	915	400	37	23	4.5	2	150	
17)	SB#36 Al_2O_3 97p.s.i.	891	340	7	23	4	2	NA	
18)	" " 97p.s.i.	891	340	7	23	4	2	NA	Minimal TiB_2 coating
19)	" " 97p.s.i.	891	340	7	23	4	2	NA	
16)	SB#36 Al_2O_3 95p.s.i.	888	866	7	23	10.4	1	62	
20)	" " 95p.s.i.	888	866	7	23	10.4	1	123	Reduced Fe_2B (porous) coating
21)	" " 95p.s.i.	888	866	7	23	10.4	1	93	

Above specimens are all incompletely coated, gas exit ends are not coated.

APPENDIX E - RESULTS OF CVD TiB_2 COATING (Preliminary Runs)

Substrate Materials: 1040 C.S. (0.4%C, 1.2%Mn)

Substrate Dimensions: (width x length x thickness) 33.3mm x 31.8mm x 0.79mm

Spec. No.	Surface Preparation	Temp. °C	H_2 flow ml/min.	BCl_3 flow ml/min.	$TiCl_4$ Temp. °C	$TiCl_4$ Flow ml/min.	Duration Hr.	Wt. Gain mg.	Remarks
22)	SB#36 Al_2O_3 95p.s.i.	888	866	0	NA	0	1½	(16)*	
23)	" " 95p.s.i.	888	866	0	NA	0	1½	(2)	Uncoated specimens
24)	" " 95p.s.i.	888	866	0	NA	0	1½	(33)	
34)	SB#36 Al_2O_3 95p.s.i. Electroless Ni plated	970	866	22	40	26.2	1½	162	Less porosity
37)	SB#36 Al_2O_3 95p.s.i.	970	866	22	40	26.2	1½	(150	High porosity
38)	SB#36 Al_2O_3 95p.s.i.	925	866	22	40	26.2	2	259	Completely coated with
39)	" " 95p.s.i.	925	866	22	40	26.2	2	(10)	TiB_2 and Fe_2B (porous)
40)	" " 95p.s.i.	925	866	22	40	26.2	2	(6)	
41)	SB#36 Al_2O_3 95p.s.i. CVD TIC Coated	925	866	24	40	26.2	2	419	Improved coating adhesion, no porosity, evenly and completely coated.
42)	SB#36 Al_2O_3 95p.s.i. CVD TIC Coated	925	866	24	40	26.2	2	468	
43)	SB#36 Al_2O_3 95p.s.i.	925	866	11	40	26.2	2	303	Reduced Fe_2B (porous)
44)	" " 95p.s.i.	925	866	11	40	26.2	2	262	
45)	SB#36 Al_2O_3 95p.s.i.	941	866	7	40	26.2	2	138	Centre specimen and side
46)	" " 95p.s.i.	941	866	7	40	26.2	2	111	specimens inner sides uncoated
47)	" " 95p.s.i.	941	866	7	40	26.2	2	127	(dark blue) Three specimens per run.
48)	SB#36 Al_2O_3 95p.s.i.	925	866	7	40	26.2	2	364	Good sound coating without
49)	" " 95p.s.i.	925	866	7	40	26.2	2	325	porosity
50	SB#36 Al_2O_3 95p.s.i.	925	866	7	40	26.2	2	251	Single specimen per run
52)	SB#36 Al_2O_3 95p.s.i.	925	866	7	40	26.2	2	300	Two specimens per rim
53)	" " 95p.s.i.	925	866	7	40	26.2	2	NA	
54)	SB#36 Al_2O_3 95p.s.i.	1000	866	7	40	26.2	2	168	Two specimens per run
55)	" " 95p.s.i.	1000	866	7	40	26.2	2	157	

* () less weight.

APPENDIX E - RESULTS OF CVD TiB_2 COATING

Substrate Materials: 1040 C.S. (0.4%C, 1.2%Mn)

Substrate Dimensions: 30mm x 25mm x 0.76mm
(width x length x thickness) A Group: 30mm x 25mm x 3.18mm (1018 C.S.)

Spec. No.	Surface Preparation	Temp. °C	H_2 flow ml/min.	BCl_3 flow ml/min.	$TiCl_4$ Temp. °C	$TiCl_4$ Flow ml/min.	Duration Hr.	Wt. Gain mg.	Remarks
1	SB#36 Al_2O_3 95p.s.i.	927	890	7	45	34.2	2	219	Yellow discoloration
2	" " 95p.s.i.	927	890	7	45	34.2	2	195	
3	" " 95p.s.i.	927	890	7	45	34.2	NA	NA	Gas line blockage
4	" " 95p.s.i.	927	890	7	45	34.2	2	258	Graphite suceptor moved forward Gas flow pattern unchanged
6	" " 95p.s.i.	927	890	7	45	34.2	2	154	BCl_3 left on for 30 min. (after coating) dots on gas flow pattern
8	" " 95p.s.i.	927	890	7	45	34.2	2	176	Overnight Hydrogen flush
5)	" " 95p.s.i.	927	890	7	45	34.2	2	231	Tandem specimens showing
7)	" " 95p.s.i.	927	890	7	45	34.2	2	31	gas flow pattern
9)	" " 95p.s.i.	927	890	7	45	34.2	2	276	Tandem specimens showing
10)	" " 95p.s.i.	927	890	7	45	34.2	2	66	gas flow pattern
11	" " 95p.s.i.	927	890	7	45	34.2	2	264	
12	" " 95p.s.i.	927	890	7	45	34.2	NA	NA	Gas line blockage
13	" " 95p.s.i.	927	890	7	45	34.2	2	184	Yellow discoloration at gas entrance
14	" " 95p.s.i.	927	890	6.9	45	34.2	2	270	initial coating, BCl_3 only for 3mi
15	" " 95p.s.i.	927	890	6.5	45	34.2	2	218	BCl_3 flowmeter malfunction
16	" " 95p.s.i.	927	890	6.9	45	34.2	2	318	
17	" " 95p.s.i.	927	890	6.9	45	34.2	2	NA	
18	" " 95p.s.i.	927	890	4.3	45	34.2	2	114	Generator failure
21	" " 95p.s.i.	927	890	5.5	45	34.2	3	228	Coating flaked off at gas entry end and edges
22	" " 95p.s.i.	927	890	6.9	45	34.2	2½	296	Coating flaked off
23	" " 95p.s.i.	927	890	6.9	45	34.2	3	477	
25	" " 95p.s.i.	927	890	6.9	45	34.2	3	486	
26	" " 95p.s.i.	927	890	6.9	45	34.2	2½	417	
A3	" " 95p.s.i.	927	890	6.9	45	34.2	2	221	Coating flaked off at gas entry end and edges

APPENDIX E - RESULTS OF CVD TiB_2 COATING

Substrate Materials: 430 S.S. (0.12%C, 1.0%Mn, 16-18%Cr)

Substrate Dimensions: (width x length x thickness) 30mm x 25mm x 0.76mm

Spec. No.	Surface Preparation	Temp. °C	H_2 flow ml/min.	BCl_3 flow ml/min.	$TiCl_4$ Temp. °C	$TiCl_4$ Flow ml/min.	Duration Hr.	Wt. Gain mg.	Remarks
B 1	SB#36 Al_2O_3 95p.s.i.	927	890	6.9	45	34.2	2	NA	Coating flaked off, BCl_3 too high
2	" " 95p.s.i.	927	890	6.9	45	34.2	2	195	Coating flaked off at gas entry end
3	" " 95p.s.i.	927	890	4.3	45	34.2	½	NA	
4	" " 95p.s.i.	927	890	4.3	45	34.2	2	178	Generator shut off twice
5	" " 95p.s.i.	927	890	4.3	45	34.2	NA	NA	Generator malfunction
6	" " 95p.s.i.	927	890	5.5	45	34.2	2	198	Dots on coating
7	" " 95p.s.i.	927	890	6.9	45	34.2	2	218	Coating flaked off at gas entry end
8	" " 95p.s.i.	927	890	4.3 - 5.5	45	34.2	3	325	
9	" " 95p.s.i.	927	890	4.3	45	34.2	3	284	
10	" " 95p.s.i.	927	890	4.3 - 5.5	45	34.2	3	354	
11	" " 95p.s.i.	927	890	4.3	45	34.2	2	NA	
13	" " 95p.s.i.	927	890	4.3	45	34.2	2	208	
14	" " 95p.s.i.	927	890	5.5	45	34.2	3	320	Flaking at gas entry end.
17	" " 95p.s.i.	927	890	4.3 - 5.5	45	34.2	3	307	Dots on coating
19	" " 95p.s.i.	927	890	4.3	45	34.2	3	245	Dots on coating
20	" " 95p.s.i.	927	890	4.3 - 5.5	45	34.2	3	328	
21	" " 95p.s.i.	927	890	4.3 - 5.5	45	34.2	3	255	Coating flaked at gas entry end.
23	" " 95p.s.i.	927	890	4.3 - 5.5	45	34.2	3	281	" " " " " "
24	" " 95p.s.i.	927	890	4.3 - 5.5	45	34.2	3	291	" " " " " "
26	" " 95p.s.i.	927	890	4.3 - 5.5	45	34.2	3	264	" " " " " "
27	" " 95p.s.i.	927	890	4.3 - 5.5	45	34.2	3	237	" " " " " "
28	" " 95p.s.i.	927	890	4.3 - 5.5	45	34.2	3	294	" " " " " "
29	" " 95p.s.i.	927	890	4.3	45	34.2	3	299	" " " " " "
31	" " 95p.s.i.	927	890	4.3 - 5.5	45	34.2	3	115	Entrance flaked off
33	" " 95p.s.i.	927	890	4.3 - 5.5	45	34.2	3	272	" " "
34	" " 95p.s.i.	927	890	4.3 - 5.5	45	34.2	3	124	" " "
X	#60 Emery Paper	927	890	4.3	45	34.2	2	155	Coating peeled off
2X	#60 Emery Paper	927	890	4.3	45	34.2	3	NA	" " "

APPENDIX E - RESULTS OF CVD TiB_2 COATING

Substrate Materials: 304 S.S. (.08%C, 2%Mn, 18-20% Cr, 8-10.5% Ni)

Substrate Dimensions: (width x length x thickness) 30mm x 25mm x 0.76mm

Spec. No.	Surface Preparation	Temp. °C	H_2 flow ml/min.	BCl_3 flow ml/min.	$TiCl_4$ Temp. °C	$TiCl_4$ Flow ml/min.	Duration Hr.	Wt. Gain mg.	Remarks
N1	Electro-dull Ni plated	927	890	4.3	45	34.2	2	207	Shiny and smooth coating
2	" " " "	927	890	4.3	45	34.2	3	317	" " " "
3	" " " "	927	890	4.3	45	34.2	3	302	" " " "
4	" " " "	927	890	4.3	45	34.2	3	246	Crystal-like coating
5	" " " "	927	890	4.3	45	34.2	3	470	" " "
6	" " " "	927	890	4.3	45	34.2	3	434	" " "
7	Electroless Ni plated	927	890	4.3	45	34.2	3	286	No coherent coating
8	" " "	927	890	4.3	45	34.2	3	242	" " "
F1	SB#36 Al_2O_3 95p.s.i.	927	890	4.3	45	34.2	3	45	" " "
	Other Substrates								
oCr	SB#36 Al_2O_3 95p.s.i.	927	890	4.3	45	34.2	3	14	No coherent coating
6 SS	" "	927	890	6.9	45	34.2	2	57	" " "
conel	" "	927	890	4.3	45	34.2	3	13	" " "
601	" "	927	890	4.3	45	34.2	3	44	" " "

APPENDIX E - RESULTS OF CVD TiB_2 COATING

Substrate Materials: 410 S.S. (,15%C, 1%Mn, 11.5-13.5% Cr)

Substrate Dimensions: (width x length x thickness) 30mm x 25mm x 1.83mm

Spec. No.	Surface Preparation	Temp. °C	H_2 flow ml/min.	BCl_3 flow ml/min.	$TiCl_4$ Temp. °C	$TiCl_4$ Flow ml/min.	Duration Hr.	Wt. Gain mg.	Remarks
C 1	SB#36 Al_2O_3 95p.s.i.	927	890	4.3	45	34.2	3½	238	Coating flaked at gas entry end.
2	" " 95p.s.i.	927	890	4.3	45	34.2	3	327	
3	" " 95p.s.i.	927	890	4.3	45	34.2	3	334	Coating flaked at gas entry end.
4	" " 95p.s.i.	927	890	4.3	45	34.2	3	332	" " " " " "
5	" " 95p.s.i.	927	890	4.3 - 5.5	45	34.2	2½	324	" " " " " "
6	" " 95p.s.i.	927	890	2.2	45	34.2	3	196	Uncoated at exit corners
7	" " 95p.s.i.	927	890	3.3	45	34.2	3	169	" " " "
8	" " 95p.s.i.	850	890	4.3	45	34.2	3	63	Coating flaked off
9	" " 95p.s.i.	1000	890	4.3	45	34.2	3	225	Uncoated at top and bottom
10	" " 95p.s.i.	927	890	4.3	45	34.2	3	348	
11	" " 95p.s.i.	927	890	4.3	45	34.2	3	(2822)	Specimen corroded
12	" " 95p.s.i.	927	890	4.3	45	34.2	3	107	Coating flaked off

APPENDIX "F" - EFFICIENCY OF TiB_2 FORMATION

Molecular Weight of TiB_2, solid, (s)	69.52
Molecular Weight of $TiCl_4$:	189.73
Density of $TiCl_4$, liquid, (l):	1.726 gm/ml
Temperature of $TiCl_4$ chamber water bath:	318^oK (45^oC)
Flow rate of $TiCl_4$, gas, (g)	34.2 ml/min.
Average Consumption of $TiCl_4$ (l)	30 ml/3 hr.run
Deposition time:	180 min. (3 hrs)
Average weight gain of substrate TiB_2):	0.4 gm.

No. of moles of $TiCl_4$ (g) consumed:
(assume ideal gas law)

$$N_1 = \frac{PV}{RT} = \frac{1 \times 34.2 \times 180 \times 10^{-3}}{0.082 \times 318}$$

$$= 0.236.$$

Compared with No. of moles of $TiCl_4$ (l) evaporated.

$$N_2 = \frac{30 \times 1.726 \times 10^{-3}}{189.73}$$

$$= 0.273 \quad \text{(compared with 0.236)}$$

APPENDIX "F" - EFFICIENCY OF TiB_2 FORMATION - continued

No. of moles of TiB_2 (s) deposited

$$N_3 = \frac{0.4}{69.52} = 0.00575$$

$\therefore$ Efficiency of TiB_2 formation:

$$\frac{N_3}{N_2} \times 100\% = \frac{0.00575}{0.273} \times 100\%$$

$$= 2.1\%$$

LIST OF FIGURES

FIGURE 1 : Schematic Diagram of Cold Wall CVD Circuit

2 : CVD Apparatus with metal chamber

3 : Graphite Susceptor

4 : Metal Chamber

5 : Surface markings on coated specimens showing regions A, B and C.

6 : SEM of Region A

7 : SEM of Region B

8 : SEM of Region C

9 : SEM of TiB_2 coating (shiny) on dull-Ni plated 304 S.S.

10 : SEM of TiB_2 coating (dull) on dull-Ni plated 304 S.S.

11 : Coating distribution across the substrate

12 : TiB_2 coating on 1040 C.S.

(a) Unetched

(b) Etched in 2% nital

13 : TiB_2 coating on 410 S.S. (Similar to 430 S.S.)

(a) Unetched

(b) Etched in Villelas Reagent

14 : TiB_2 coating on dull-Ni plated 304 S.S.

(a) Unetched

(b) Etched in 10% Oxalic acid

15 : Porous Fe_2B interface between TiB_2 and 1040 C.S.

(a) Unetched

(b) Etched in 2% nital

16 : SEM of TiB_2 coated 1040 C.S.

17 : SEM of TiB_2 coated 430 S.S.

18 : SEM of TiB_2 on dull-Ni plated 304 S.S.

19 : SEM of Porous Fe_2B interface on 1040 C.S.

20 : Corrosion Tests

(a) Top Row - 1040 C.S., 430 S.S. 410 S.S. (coated)
Bottom Row - 1040 C.S., 430 S.S., 410 S.S. (uncoated)

(b) 304 S.S. (bare) dull nickel plated 304 S.S., dull nickel plated 304 S.S. with TiB_2 coating.

21 : Bend Tests of coated specimens

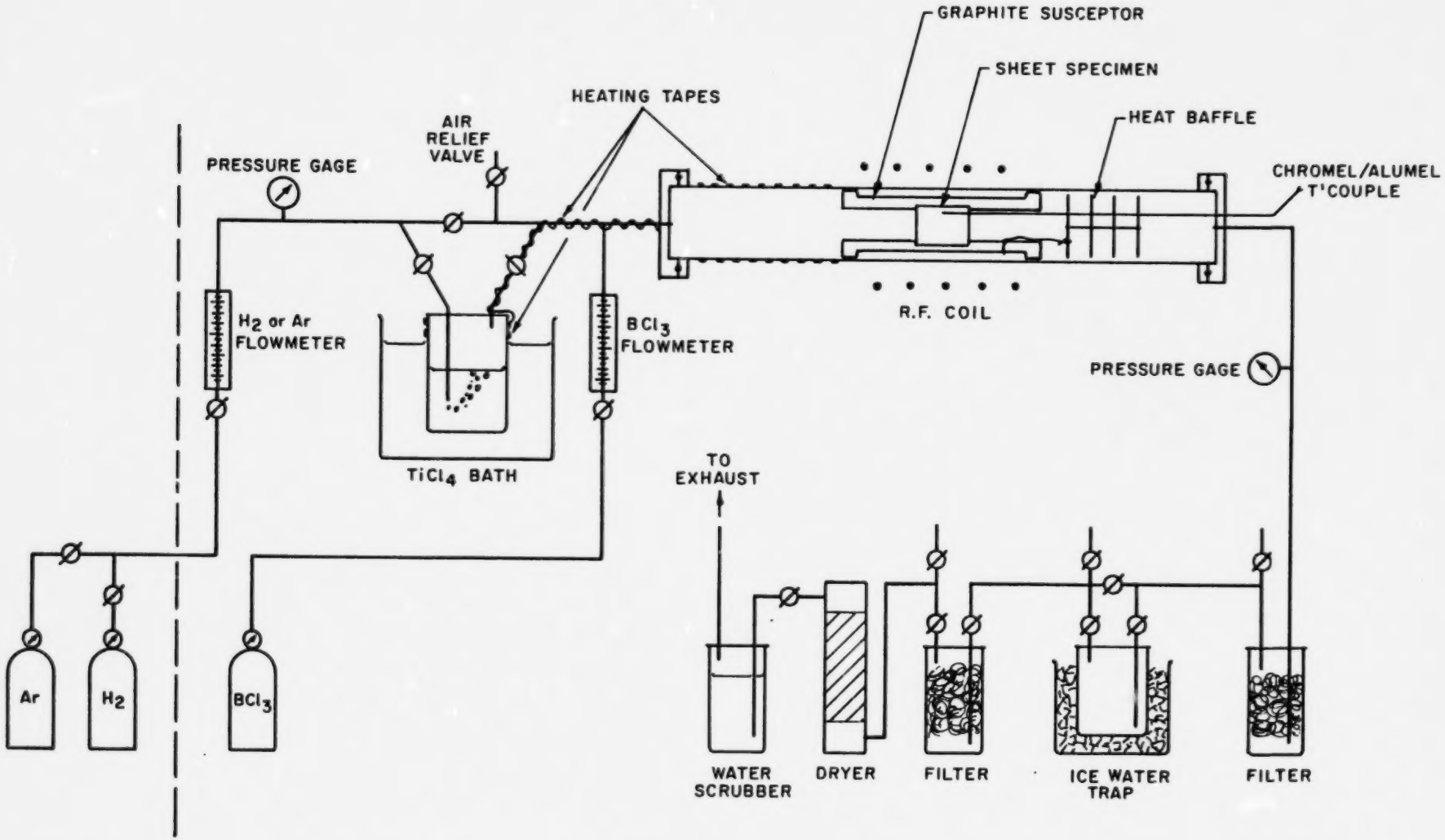

FIG. 1 SCHEMATIC DIAGRAM OF COLD WALL CVD CIRCUIT

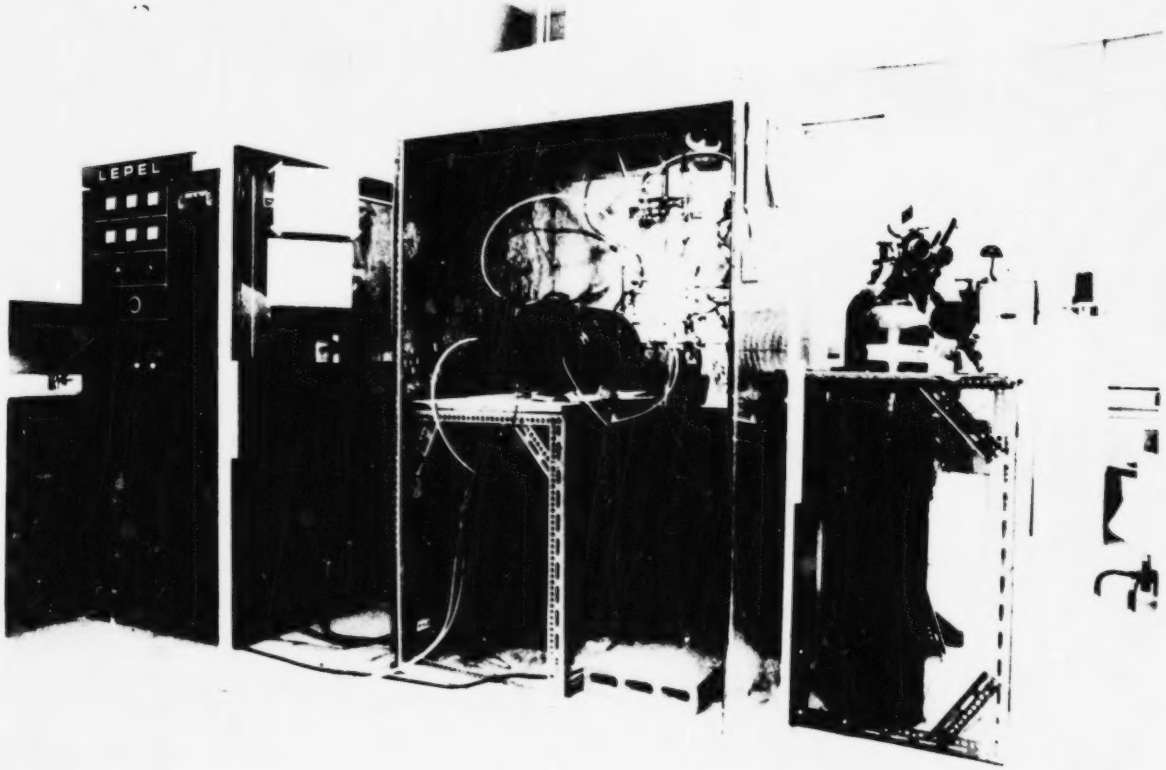

FIGURE 2.

CVD Apparatus with metal chamber.

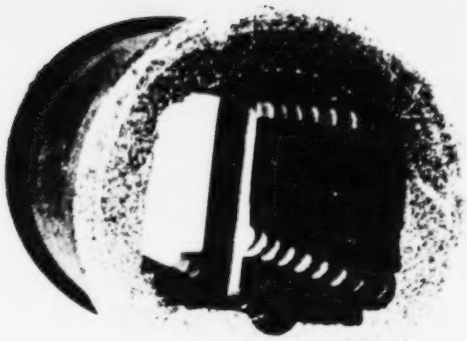

FIGURE 3. - Graphite Susceptor

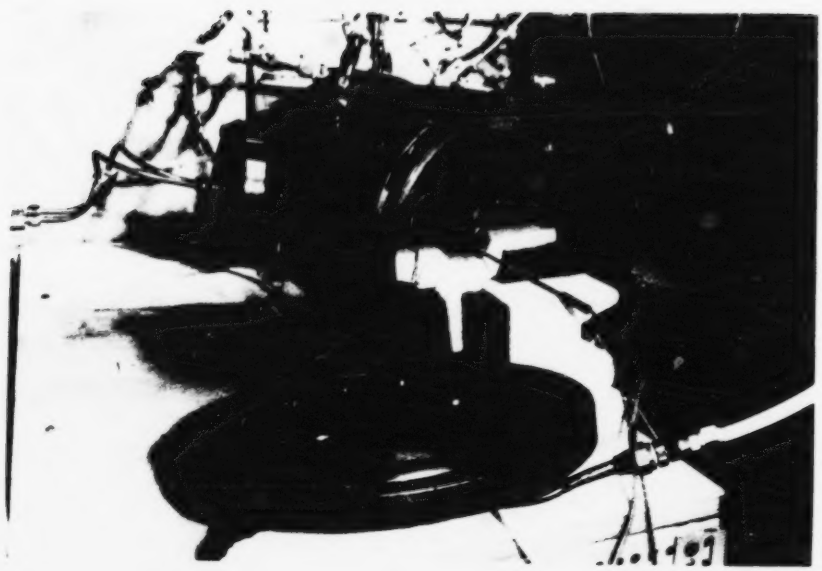

FIGURE 4. - Metal Chamber

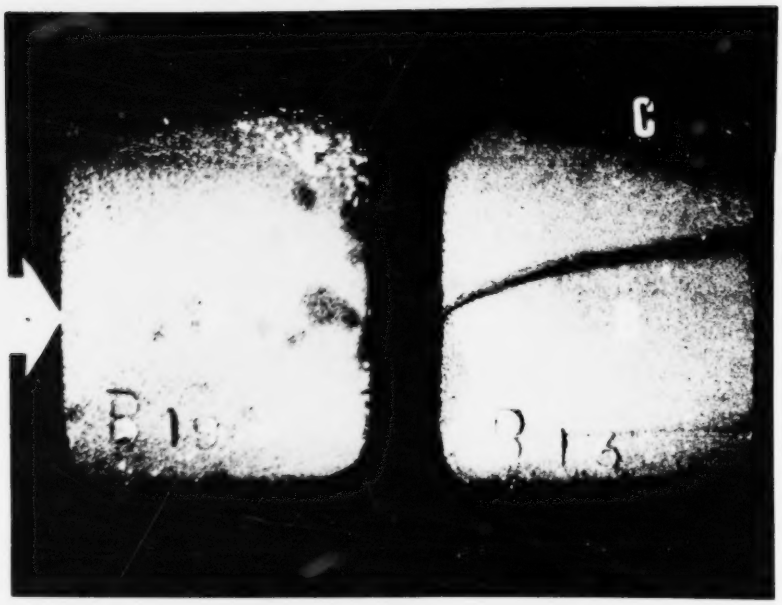

FIGURE 5. - Surface markings on coated specimens showing regions A, B and C. (Arrow indicates gas flow direction)

Figure 6. - SEM of Region A.

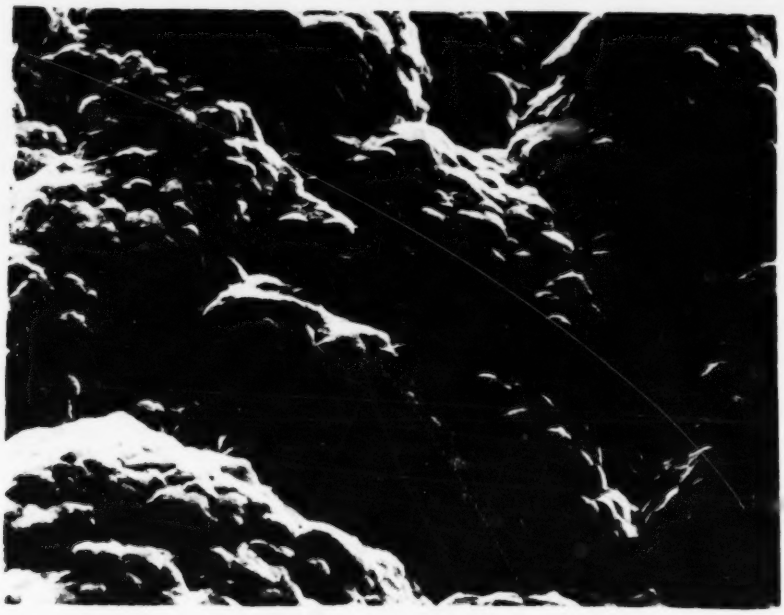

FIGURE 7. - SEM of Region B

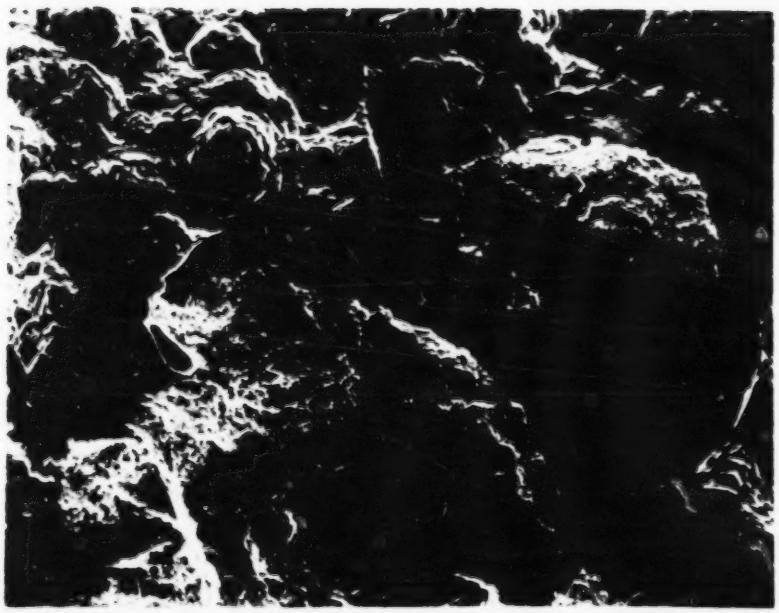

FIGURE 8. - SEM of Region C

FIGURE 9. - SEM of TiB_2 coating (shiny) on dull-Ni plated 304 S.S.

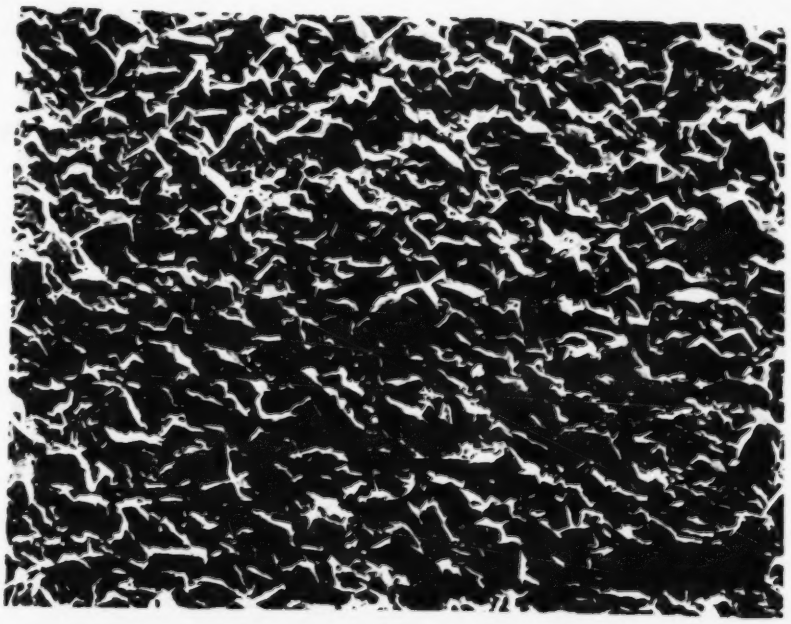

FIGURE 10. - SEM of TiB_2 coating (dull) on dull-Ni plated 304 S.S.

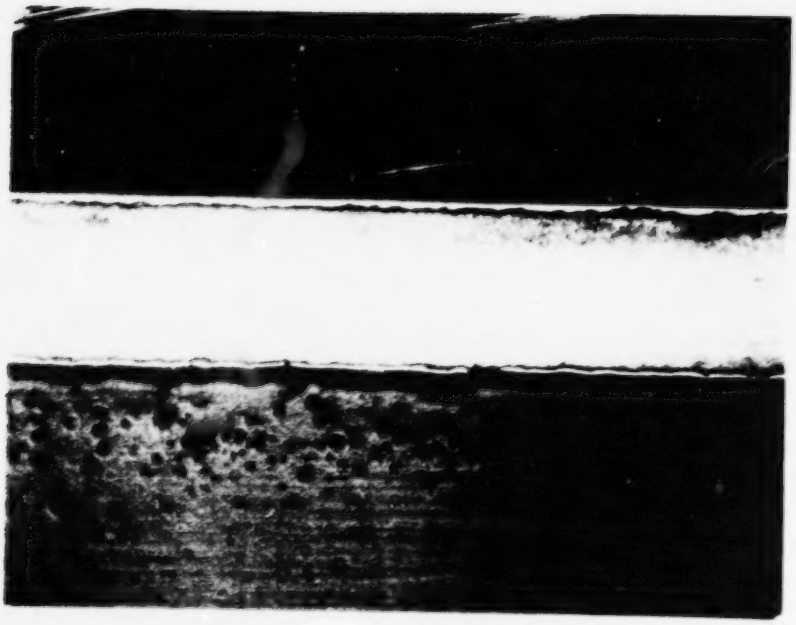

FIGURE 11. - Coating distribution across the substrate*

Mag. X30

* The bottom coating was damaged during the metallographic specimen preparation procedure.

(a) unetched

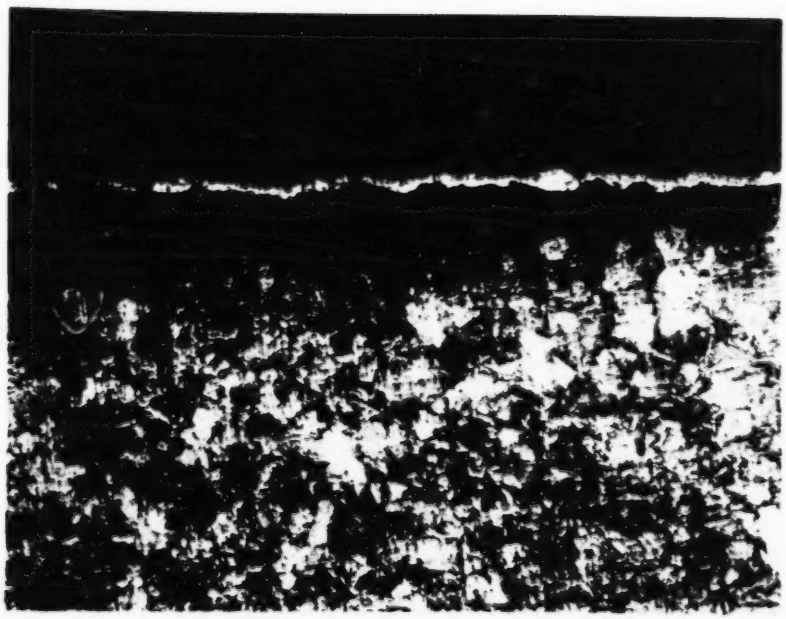

(b) etched in 2% nital.

FIGURE 12. - TiB_2 coating on 1040 C.S.

Mag. X100

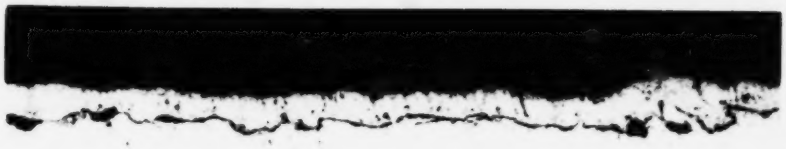

(a) unetched

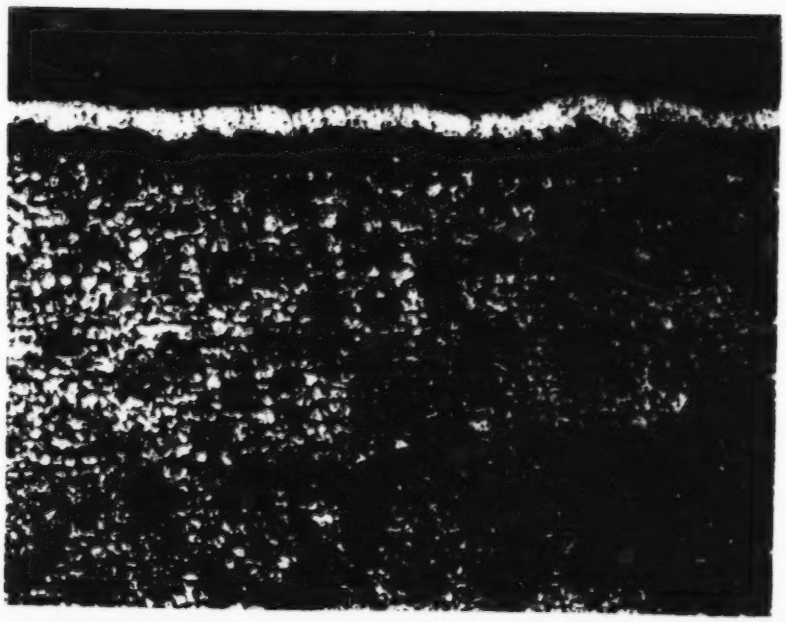

(b) Etched in Villelas

(Picric Acid 1gm)
(HCl 5ml)
(Ethyl Alcohol 100ml)

FIGURE 13. - TiB_2 coating on 410 S.S. (Similar to 430 S.S.)

Mag. X100

(a) Unetched

(b) Etched in 10% Oxalic acid

FIGURE 14. - TiB_2 coating on dull-Ni plated 304 S.S.

Mag. X100

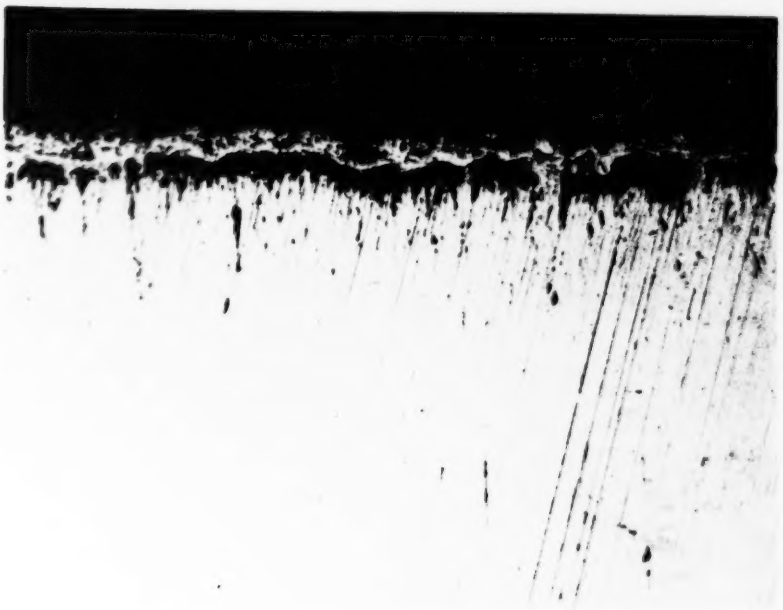

(a) Unetched

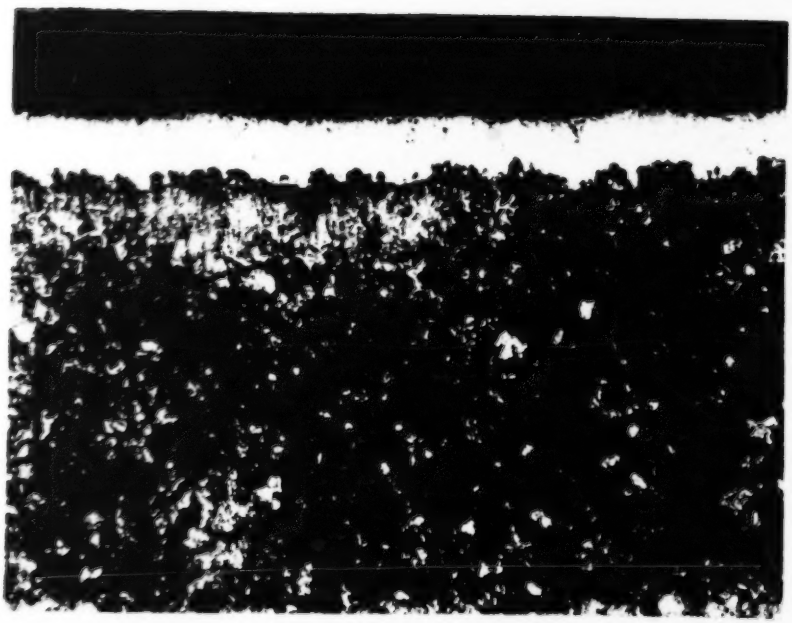

(b) Etched in 2% Nital

FIGURE 15. - Porous Fe_2B interface between TiB_2 and 1040 C.S.

Mag. X100

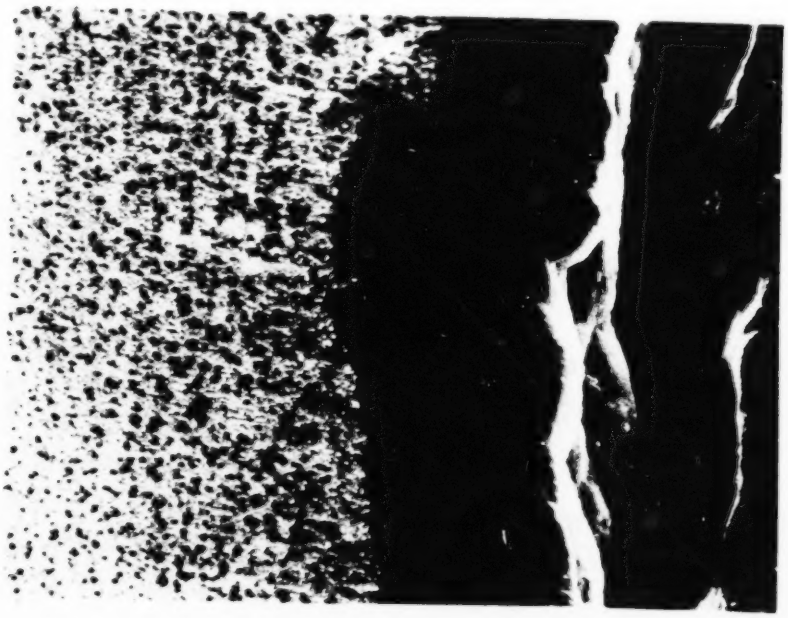

FIGURE 16. - SEM of TiB_2 coated 1040 C.S.

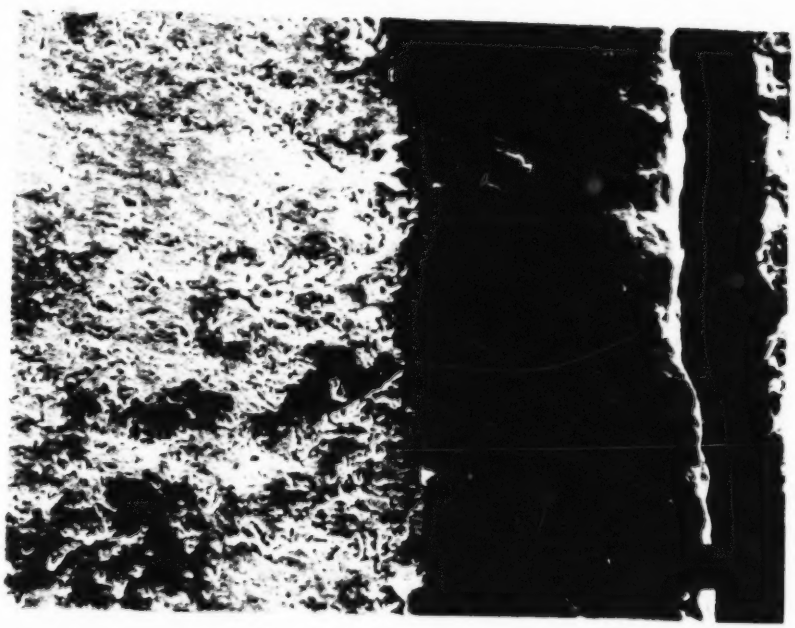

FIGURE 17. - SEM of TiB_2 coated 430 S.S.
(similar to 410 S.S.)

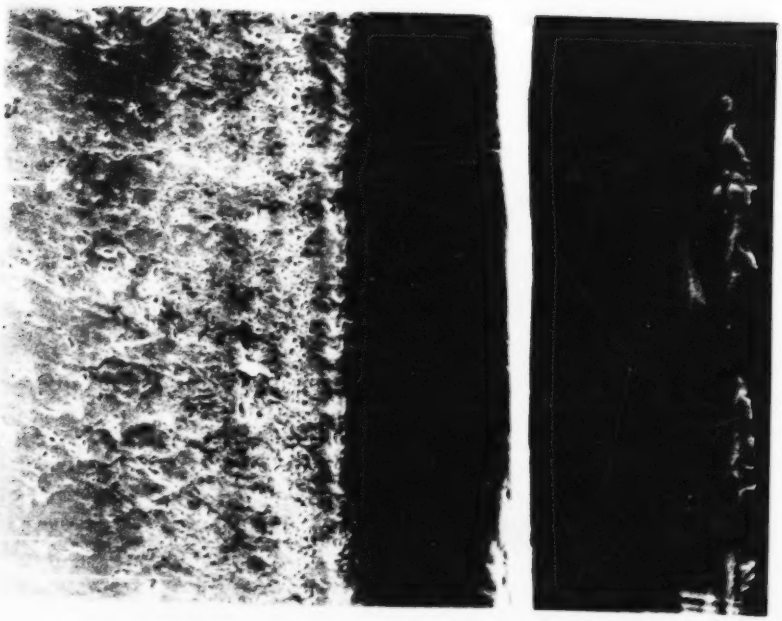

FIGURE 18. - SEM of TiB_2 on dull-Ni plated 304 S.S.

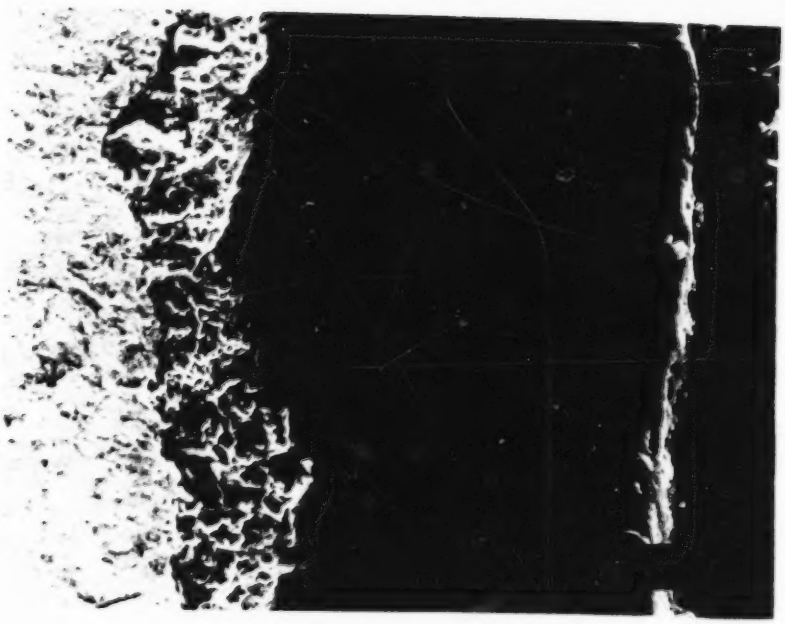

FIGURE 19. - SEM of Porous Fe_2B interface on 1040 C.S.

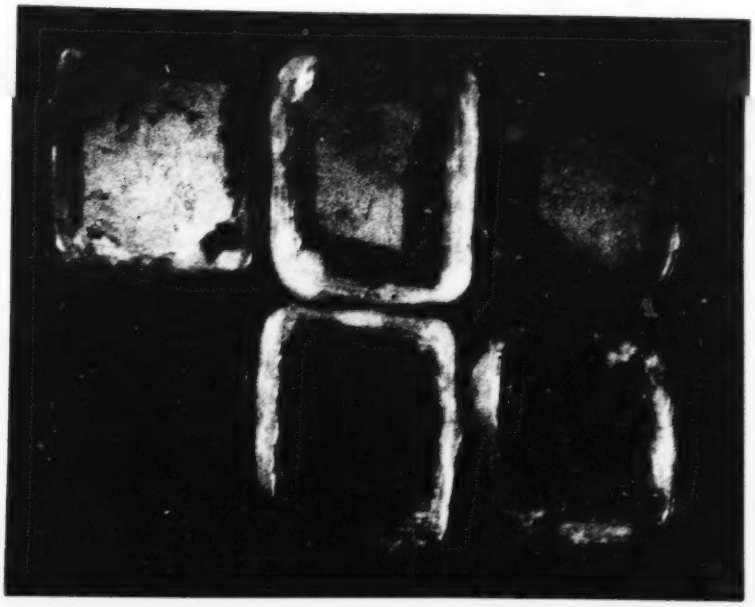

(a) Top row (from left to right) : 1040 C.S., 430 S.S., 410 S.S. (all TiB_2 coated)

Bottom row (from left to right) : 1040 C.S., 430 S.S. 410 S.S. (all uncoated)

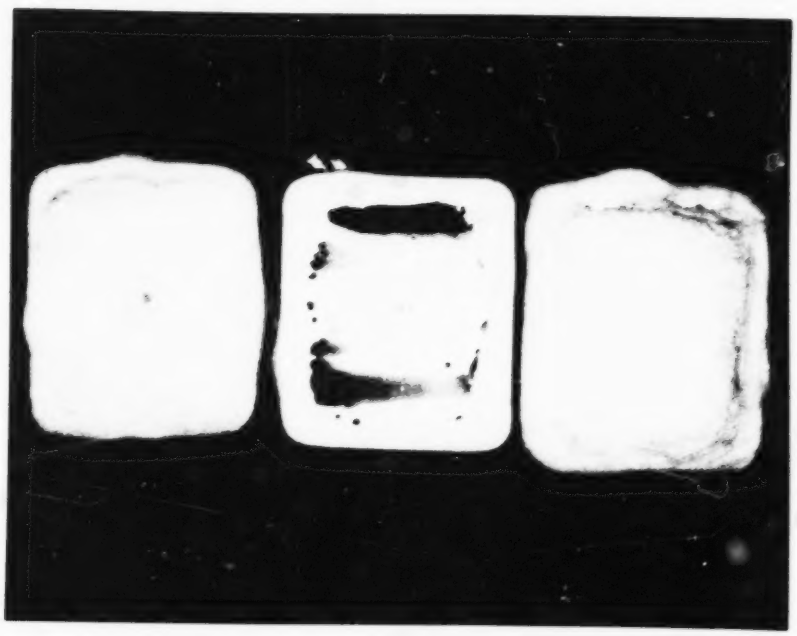

(b) 304 S.S. (bare), dull nickel plated 304 S.S., dull nickel plated 304 S.S. with TiB_2 coating. (from left to right)

FIGURE 20. - Corrosion Tests

FIGURE 21. - Bend tests of coated specimens
1040 C.S., 304 S.S. (shiny), 304 S.S. (dull),
430 S.S., 410 S.S. (from left to right)

ONTARIO RESEARCH FOUNDATION

energy conservation programs and analysis, thermal insulation design and evaluation, waste heat recovery, building energy systems and monitoring, heat storage systems, thermoelectric generation, combustion technology, burner development, heat transfer analysis, solar systems monitoring, National Solar Test Facility, solar technology, wind power, coal and lignite processing, alternate fuel utilization, battery technology, energy and chemicals from biomass, . . .

ambient air quality assessment, source sampling, odour emission and control, asbestos measurement and control, pesticide residues, trace metal analysis, trace organic analysis, mutagenic testing, occupational health surveys and assessments, water surveys, water purification, municipal and industrial waste water treatment processes, membrane separation techniques, wet oxidation, diesel emission control technology, solid waste treatment and recovery, noise and vibration analysis, environmental impact assessments, long-range transport of atmospheric pollutants, radiation measurements, particulate identification and measurement, ergonomics and industrial design, air pollution control technology, hazardous and toxic materials and waste control, . . .

building materials, plastics, coatings and composites, metals, glass and ceramics, wood and wood composites, biomaterials, adhesives and printing inks, yarns, fabrics and geotextiles, leather, organic and inorganic chemicals, specialty formulations, specification development, quality control, mechanical chemical and thermal properties, test method development, failure analysis, fire and flammability, glass-metal seals, metal and alloy powders, metallography, materials characterization by electron microscopy and X-ray microanalysis, photovoltaics and ionic conductors, corrosion properties and control, rubber technology, energy radiography, non-destructive testing, X-ray analysis, cement and concrete, gypsum, . . .

pulp and paper products, clothing, footwear and industrial textile products, knitting technology, thin and thick film systems, electronic devices, microcomputer systems and applications, fibre optics, electronic design, bioengineering, ultrasonic and fluid shear devices, microwave drying, transportation and equipment testing, mathematical stress and vibration analysis, product, equipment and machinery design and development, fuel emulsification, chemistry of foodstuffs, pulping and papermaking processes, ceramics processing, metallurgical process development, powder metal technology, packaging applications, technical and economic evaluations, industrial engineering applications, electroplating, radioactive decontamination, process control, biotechnology, industrial microbiology, enzyme analysis, cryogenics, electrical testing, . . .

mineral processing, hydro and pyrometallurgical processing of ferrous and non-ferrous ores, coal evaluation and processing, asbestos processing and applications, uranium processing, forest utilization, utilization of forest and agricultural wastes, utilization of industrial mining and domestic wastes, energy and chemicals from biomass, non-metallic minerals, . . .

ONTARIO RESEARCH FOUNDATION • SHERIDAN PARK, MISSISSAUGA, ONTARIO, CANADA L5K 1B3 • (416) 822-4111 • TELEX 06-982311